Precision Telescope Control System

PTCS/SN/3: Scientific Requirements for High-Frequency Observations with the GBT

Version:	2
Date:	2003 March 18
Authors:	J. J. Condon
Archive:	PR005
File:	PROJECTS
Keys:	PTCS, requirement, specification

Revision History

Ver.	Changes	Date	Author
0	Initial Version	2003 March 12	J. J. Condon
1	Convert to PTCS format	2003 March 17	Richard Prestage
2	Add Table 2	2003 March 18	J. J. Condon

Contents

Abstract

The performance requirements for the PTCS are determined by the science goals of the GBT at the shortest wavelengths accessible through the atmosphere at Green Bank. The most important short-term requirements are rms offset-tracking errors $\sigma_2 < 3''$ and rss surface errors $\epsilon < 0.4$ mm for acceptable performance up to 52 GHz. The ultimate goals are $\sigma_2 < 1''.5$ and $\epsilon < 0.2$ mm for astronomically usable performance at 115 GHz.

1. GBT Science

The GBT is a general-purpose telescope intended to cover the entire frequency range accessible through the atmosphere at Green Bank. The scientific requirements for high aperture efficiency, low sidelobes, and small pointing errors all imply GBT dimensional tolerances which are proportional to the observing wavelength λ. Thus PTCS is driven by the goal of making astronomically useful observations at the highest frequencies accessible through the atmosphere at Green Bank.

The major scientific programs envisioned for the GBT and their frequency ranges are shown in Figure 1 (NRAO 2000) along with the "stop bands" $52 \lesssim \nu \lesssim 68$ GHz and $\nu \gtrsim 117$ GHz where the atmosphere is nearly opaque. Some of the most important science programs cannot be characterized by a single frequency—Galactic molecular spectroscopy and observations of CO at high redshifts in particular. On the other hand, the atmospheric window $30 \lesssim \nu \lesssim 40$ GHz for good continuum observations, the SiO lines at 43 and 86 GHz, and the existing VLBA capability at 86 GHz can be used to define fairly clearcut performance parameters.

The GBT currently works quite well at the H_2O $\nu \approx 22$ GHz line frequency. The next natural goal is good performance at least up to the SiO line frequencies near 43 GHz and usable performance up to the 52 GHz atmospheric cutoff. In the 68 to 117 GHz window, the ultimate goals might be usable performance at the 115 GHz CO $J = 1 - 0$ line and good performance at 86 GHz.

Some science programs require more than just "usable" or even "good" performance. For example, mapping the H I $\lambda = 21$ cm line at high Galactic latitudes, measuring Galactic magnetic fields through Zeeman splitting, and making zero-spacing maps to complement VLA data all depend on the GBT having extremely low sidelobes, a high beam efficiency, and pointing errors much smaller than the beamwidth. Accurately measuring small flux changes in variable radio sources also requires excellent pointing. Fortunately, most of the short-wavelength science indicated in Figure 1 does not place unusually strict performance demands on the GBT. Realistic estimates of the GBT and PTCS requirements implied by those programs are given below.

2. Source Tracking

Errors in tracking a point source have two bad effects: (1) loss of sensitivity and (2) uncertainty in measured flux density. Their quantitative consequences are derived in this section.

The GBT beam is nearly a circular Gaussian of diameter θ between half-power points. The relative power gain g is

$$g = \exp\left[-4\ln(2)\left(\frac{\rho}{\theta}\right)^2\right], \tag{1}$$

where ρ is the angular displacement of the beam center from a point source. The probability distribution of g is determined by the probability distribution of the tracking error ρ.

The probability distribution of beam pointing errors in one coordinate can usually be approximated by a Gaussian. Let $(\Delta x,\ \Delta y)$ be angular offsets in any pair of orthogonal coordinates $(x,\ y)$, azimuth and elevation for example. Their probability distributions can be written

$$p_{\rm x}(\Delta x) = \frac{1}{(2\pi)^{1/2}\sigma_{\rm x}} \exp\left[-\frac{(\Delta x)^2}{2\sigma_{\rm x}^2}\right] \tag{2a}$$

$$p_{\rm y}(\Delta y) = \frac{1}{(2\pi)^{1/2}\sigma_{\rm y}} \exp\left[-\frac{(\Delta y)^2}{2\sigma_{\rm y}^2}\right], \tag{2b}$$

where $\sigma_{\rm x}$ and $\sigma_{\rm y}$ are the rms one-dimensional pointing errors in the x and y directions. If the errors in x and y are uncorrelated, the joint probability $p_{\rm x,y}(\Delta x, \Delta y)$ of simultaneous offsets Δx and Δy is

$$p_{\rm x,y}(\Delta x, \Delta y) = p_{\rm x}(\Delta x) \cdot p_{\rm y}(\Delta y)\,. \tag{3}$$

Usually $\sigma_{\rm x} \approx \sigma_{\rm y}$ [see Fig. 3 in Balser et al. (2002a)] so

$$p_{\rm x,y}(\Delta x, \Delta y) = \frac{1}{2\pi\sigma_1^2} \exp\left[-\frac{(\Delta x)^2 + (\Delta y)^2}{2\sigma_1^2}\right], \tag{4}$$

where $\sigma_1 \approx \sigma_{\rm x} \approx \sigma_{\rm y}$ is the rms one-dimensional pointing error. The tracking error

$$\rho = [(\Delta x)^2 + (\Delta y)^2]^{1/2} \tag{5}$$

is the two-dimensional pointing error. The probability distribution of ρ deduced from

$$p_\rho(\rho)d\rho = p_{\rm x,y}(\Delta x, \Delta y)2\pi\rho d\rho \tag{6}$$

is the (very non-Gaussian) Rayleigh distribution

$$p_\rho(\rho) = \frac{\rho}{\sigma_1^2} \exp\left(-\frac{\rho^2}{2\sigma_1^2}\right). \tag{7}$$

The mean squared tracking error $\langle\rho^2\rangle$ is

$$\langle\rho^2\rangle \equiv \sigma_2^2 = \int_0^\infty \rho^2 p_\rho(\rho)d\rho = 2\sigma_1^2\,. \tag{8}$$

The phrase "rms pointing error" usually means the rms pointing error in two dimensions σ_2. For example, the GBT construction contract defined the pointing error as "the difference between the commanded position of the antenna and the actual sky position of the main beam of the antenna" (Hall et al. 1993). It is important to distinguish between the one-dimensional error σ_1 from the two-dimensional error σ_2. For example, the "rms variation of the telescope beam on the sky" measured by tracking a source at a

point on the half-power circle of the GBT beam (Balser et al. 2002b) is actually σ_1 because small pointing errors in the direction perpendicular to the line between the source and beam axis are not observable by that technique.

The differential probablity distribution of on-source gain g is related to the tracking error distribution $p_\rho(\rho)$ by

$$|p_g(g)dg| = |p_\rho(\rho)d\rho| \,. \tag{9}$$

Since $p_g(g)$ is normalized, the average gain in the source direction is

$$\langle g\rangle \equiv \int_0^1 g p_g(g)dg = \int_0^\infty g(\rho)p_\rho(\rho)d\rho \tag{10a}$$

$$\langle g\rangle = \int_0^\infty \exp\left[-4\ln(2)\left(\frac{\rho}{\theta}\right)^2\right]\frac{\rho}{\sigma_1^2}\exp\left(-\frac{\rho^2}{2\sigma_1^2}\right)d\rho \tag{10b}$$

$$\langle g\rangle = \left[1+\frac{8\ln(2)\sigma_1^2}{\theta^2}\right]^{-1} = \left[1+\frac{4\ln(2)\sigma_2^2}{\theta^2}\right]^{-1} \tag{10c}$$

The normalized pointing parameter z defined by

$$z \equiv 4\ln(2)\left(\frac{\sigma_2}{\theta}\right)^2 \tag{11}$$

is a convenient figure-of-merit specifying the pointing accuracy needed to maximize the on-source gain and minimize the uncertainty in on-source gain. The dimensionless ratio of rms pointing error to half-power beam diameter

$$f \equiv \left(\frac{\sigma_2}{\theta}\right) \tag{12}$$

is also frequently used to describe pointing accuracy. In terms of z,

$$\langle g\rangle = (1+z)^{-1} \,. \tag{13}$$

For many observing programs, the effect of gain loss on sensitivity can be overcome by additional integration; the relative integration time τ must be

$$\tau \approx \langle g\rangle^{-2} = (1+z)^2 \,. \tag{14}$$

The fractional increase $\Delta\tau$ in integration time needed to compensate for tracking errors is plotted as a function of f in Figure 2.

Next we derive the intensity-proportional flux uncertainty caused by tracking errors. The variance in g is

$$\sigma_g^2 \equiv \langle g^2\rangle - \langle g\rangle^2 \,, \tag{15}$$

where

$$\langle g^2\rangle \equiv \int_0^1 g^2 p_g(g)dg = \int_0^\infty g^2 p_\rho(\rho)d\rho \,. \tag{16a}$$

$$\langle g^2\rangle = \int_0^\infty \exp\left[-8\ln(2)\left(\frac{\rho}{\theta}\right)^2\right]\frac{\rho}{\sigma_1^2}\exp\left(-\frac{\rho^2}{2\sigma_1^2}\right)d\rho \tag{16b}$$

$$\langle g^2 \rangle = \left[1 + \frac{16\ln(2)\sigma_1^2}{\theta^2}\right]^{-1} = (1+2z)^{-1} \tag{16c}$$

Thus

$$\sigma_g^2 = (1+2z)^{-1} - (1+z)^{-2} . \tag{17}$$

Since $\langle g \rangle < 1$, observed intensities must be divided by $\langle g \rangle$ to yield unbiased estimates of the source flux density S. The rms fractional uncertainty in estimates of S caused by pointing errors is

$$\sigma_s = \frac{\sigma_g}{\langle g \rangle} = \frac{z}{(1+2z)^{1/2}} . \tag{18}$$

Figure 2 shows the variation of the fractional flux error σ_s with f, the rms tracking error in beamwidths. The distribution of on-source gain is

$$p_g(g) = p_\rho(\rho)|dg/d\rho|^{-1} = \frac{g^{(1-z)/z}}{z} \qquad (0 < g < 1) , \tag{19}$$

which is very skewed. The corresponding distribution of the unbiased flux-density estimator $s = g/\langle g \rangle$ caused by pointing errors is

$$p_s = p_g|ds/dg|^{-1} = \frac{s^{-(1+z)/z}}{z(1+z)^{1/z}} \qquad (0 < s < 1+z) . \tag{20}$$

The distribution of s is plotted in Figure 3 for several values of f, the tracking error in beamwidths.

The long tails of p_s and p_g are a problem for reliable detection experiments such as finding redshifted CO emission lines from distant galaxies—there is a small but non-negligible chance of missing a weak detection because the pointing offset happened to be large. The cumulative probability $P(< g)$ of getting an on-source gain $< g$ is

$$P(< g) = \int_0^g p_g(g')dg' = g^{1/z} . \tag{21}$$

The values of g corresponding to P = 0.01 (99% confidence) and P = 0.05 (95% confidence) are plotted as functions of $f = \sigma_2/\theta$ in Figure 4. For example, if $f = 0.2$, there is a $P = 0.01$ probability of getting $g < 0.60$. Compared with a dectection experiment having no pointing errors, the 99% confidence upper limit is a factor $g^{-1} \approx 1.67$ higher, and an integration $\tau = g^{-2} \approx 2.8$ times as long would be needed to set the same upper limit.

The bottom line is that *fluctuations* in gain have much worse consequences than the *mean* gain loss, in terms of both data quality and operational efficiency. If we require $\sigma_s \lesssim 0.1$ (10% rms flux errors) for astronomically usable performance, then the largest acceptable tracking error is

$$f \equiv \frac{\sigma_2}{\theta} \approx 0.2 . \tag{22}$$

In words, the rms offset between the commanded and actual telescope position should never exceed 0.2 beamwidths. For "good" performance (5% rms flux errors), the normalized pointing error should not be more than $f \approx 0.14$.

These tracking requirements do not imply comparable requirements for the "blind" or absolute pointing accuracy of the GBT because there are thousands of strong sources with precisely ($\sigma_2 < 1''$) known

absolute positions which can be used as offset pointing calibrators (Condon & Yin 2001). Since the GBT is so sensitive, a suitable calibrator can be found within 2° or 3° of most celestial positions north of declination $\delta = -40°$. The measured azimuth and elevation offsets of the calibrator can be applied to the observing position, so the GBT need only have good differential pointing accuracy over angular shifts of several degrees for durations equal to the time between observations of the calibrator. The principal cost of offset pointing is lowered operational efficiency, but the overhead of calibrating once every 30 or 60 minutes is small.

3. Blind Pointing

The "blind" (or absolute) pointing error is the difference between the actual and commanded position with no offset corrections derived from observations of astronomical sources. The requirement for blind pointing is set by the operational need to locate the nearest pointing calibration source quickly and reliably. For example, we might require that the calibrator pass through the half-power beam circle on at least one arm of a cross scan 99% of the time. If $\sigma_x \approx \sigma_y$, this requirement implies

$$\left[1 - \int_{-\theta/2}^{+\theta/2} p_x(x)dx\right]^2 = 0.01 \tag{23a}$$

$$\int_{-\theta/2}^{+\theta/2} \frac{1}{(2\pi)^{1/2}\sigma_1} \exp\left(-\frac{x^2}{2\sigma_1^2}\right) dx = 0.90 \tag{23b}$$

so

$$\frac{\theta/2}{\sigma_1} \approx 1.64 \tag{24}$$

and

$$f \equiv \left(\frac{\sigma_2}{\theta}\right) = \left(\frac{2^{1/2}\sigma_1}{\theta}\right) \approx 0.43\,. \tag{25}$$

The blind pointing requirement of Equation 25 is fairly stringent and may be difficult to meet at $\lambda =$ 3 mm (where $\theta \approx 7$ arcsec) without the aid of the laser rangefinders. However, it could be relaxed if more sophisticated methods than cross scans are used to locate pointing calibrators. These might include circular scans of diameter θ or even "nautilus" spiral scans.

4. Mapping

The GBT will make on-the-fly (OTF) maps with both single feeds and feed arrays. It is acceptable for the component of the *pointing* error (defined as the difference between the actual and commanded positions) parallel to the scan direction to be quite large, so long as the *position* error (defined as the difference between the actual and recorded positions) is small, or at least stable, so that the data can be gridded and convolved to form a map with small internal distortions. For example, the 300-foot telescope all-sky continuum surveys were made at the telescope slew speed by commanding the telescope to a position it could not reach during the scan. This technique covers the sky at the fastest possible rate and eliminates servo "hunting," although it has been known to shorten telescope lifetime dramatically. The GBT beam is quite small at high ($\nu \geq 30$ GHz) frequencies, so the ability to make OTF continuum

maps at a significant fraction of the slew speed without lowering the parameter Ω/σ^2 (where Ω is the solid angle covered per unit time and σ is the rms map noise) significantly (e.g., by more than 15%) will be important for covering large areas of sky (Brian Mason, private communication).

The component of the pointing error perpendicular to the OTF scan direction only affects the ability to interleave scans accurately and may be fairly large, so long as the position error is small or stable. By keeping the scan separation well below the Nyquist separation $\theta/2$ and/or using "basketweaving" techniques to help fill small gaps, most OTF observers should be able to avoid sampling problems and tolerate larger pointing errors than specified in Section 2.

5. VLBI

The GBT may be used with the VLBA to find fringes on very faint sources at frequencies up to 86 GHz. Since the observed fringe amplitude on a baseline including the GBT is proportional to the GBT voltage gain ($\propto g^{1/2}$, not power gain ($\propto g$), the effects of GBT pointing errors are reduced:

$$g^{1/2} = \exp\left[-4\ln(2)\left(\frac{\rho}{\sqrt{2}\theta}\right)^2\right]. \tag{26}$$

Thus we can use the analysis from Section 2 with $\sqrt{2}\theta$ replacing θ.

It isn't quite fair to relax the GBT pointing requirements by $\sqrt{2}$ and put all of the burden on the VLBA antennas, which have pointing errors themselves. We might instead require that the beam-normalized GBT pointing errors f not exceed the corresponding VLBA pointing errors. Since the GBT beamwidth is only $1/4$ of the VLBA beamwidth, the GBT pointing error σ_2 would have to be only $1/4$ of the VLBA pointing error, which is $\sigma_2 \approx 8''$. The ultimate pointing requirement for using the GBT with the VLBA at 86 GHz, $\sigma_2 \approx 2''$, is still somewhat less stringent than the tracking requirements already derived in Section 2.

Another VLBI requirement is inteferometric phase stability. If the ray path lengths between the reflector, subreflector, and feed changes by ϵ, the GBT phase ϕ will change by $\Delta\phi = 2\pi\epsilon/\lambda$. Since the GBT is four times as big as a VLBA antenna, passive length changes caused by gravity or temperature changes are likely to be four times as large. Active control of the GBT axial focus tracking will also introduce phase shifts.

6. Wavefront Phase Errors

Viewed as a transmitting antenna, the GBT should emit a plane wave normal to the line-of-sight. Departures of the primary and secondary reflector surfaces from their ideal shapes introduce wavefront phase errors that reduce gain and aperture efficiency, broaden the main beam, and increase sidelobe levels. If the rms departure normal to the ideal surface shape is ϵ and the error correlation length l is much smaller than the aperture diameter, the aperture efficiency is multiplied by the factor (Ruze 1966)

$$\eta_s \approx \exp\left[-\left(\frac{4\pi\epsilon}{\lambda}\right)^2\right]. \tag{27}$$

The traditional requirement on surface accuracy for good surface efficiency is

$$\epsilon < \frac{\lambda}{16} \qquad \text{so} \qquad \eta_s \approx 0.54 \, . \tag{28}$$

A looser "light bucket" criterion is that the forward gain, which is proportional to η_s/λ^2, not decline as wavelength decreases. It implies

$$\epsilon < \frac{\lambda}{4\pi} \qquad \text{so} \qquad \eta_s \approx 0.37 \, . \tag{29}$$

Much of the power lost from the main beam goes into a sidelobe "pedestal" of width

$$\theta_p \approx \frac{D\theta}{l} \, . \tag{30}$$

For example, uncorrelated setting errors of the $l \approx 2$ m panels on the $D = 100$ m GBT primary might produce a pedestal 50 times as broad as the main beam. Such a pedestal degrades images of sources larger than θ_p.

Axial and lateral defocusing contribute wavefront phase errors having correlation lengths comparable with the reflector diameter. Axial defocusing produces rotationally symmetric phase errors proportional to even powers (primarily the second power) of distance from the aperture center. The main beam broadens slightly and is surrounded by a narrow ring sidelobe. Lateral defocusing produces antisymmetric phase errors proportional to odd powers of distance from the aperture center. The first power, a linear phase gradient across the aperture, just gives a pointing error. The third power causes the main beam to broaden asymmetrically and produces a coma lobe on one side of the beam.

The GBT has two mirrors, both of which are imperfect, and collimation errors may not be negligible. Even so, we can use Equation 27 to *define* an effective rss (root sum square) surface error *epsilon*. At $\nu = 52$ GHz we get $\epsilon = 0.36$ mm from the $\epsilon < \lambda/16$ criterion, in agreement with the requirement specified by Lockman (1998). Hall et al. (1993) specify rms surface accuracies of 0.42 mm and 0.22 mm for Phases II and III; these correspond to frequency limits of 45 GHz and 85 GHz for $\epsilon = \lambda/16$. Going the upper frequency limit of the first GBT W-band receiver, we find $\epsilon = 0.204$ mm at $\nu = 92$ GHz. The highest frequency at which we might operate the GBT is $\nu \approx 115$ GHz, the CO $J = 1-0$ rest frequency and close to the atmospheric cutoff at $\nu \approx 117$ GHz. To operate with good efficiency at 92 GHz as a light bucket at 115 GHz, the GBT must have $\epsilon < 0$ 21 mm.

7. GBT Performance Requirements

This section displays the consequences of pointing errors and wavefront phase errors for the GBT. The nominal width of the GBT beam is

$$\left(\frac{\theta}{740 \text{ arcsec}}\right) \approx \left(\frac{\text{GHz}}{\nu}\right) , \tag{31}$$

where θ is the full width between half-power points and ν is the observing frequency. Figure 5 shows the rms fractional flux error σ_s as a function of frequency for several values of σ_2, the rms tracking error (two-dimensional pointing error). Figure 6 displays the average relative gain $\langle g \rangle$ as a function of

frequency for several values of σ_2 and shows for comparison the relative gains resulting from wavefront phase errors caused by reflector surface errors ϵ.

Figure 7 shows the GBT pointing requirements as functions of frequency for blind pointing ($f = 0.43$), usable tracking ($f = 0.20$), and accurate tracking ($f = 0.14$). Frequencies of particular interest include 52 GHz, the upper limit of the Q-band receiver and that atmospheric window, 92 GHz, the upper limit of the first GBT W-band receiver, and 115 GHz, the CO $J = 1 - 0$ line frequency and upper limit to the 3 mm atmospheric window.

The main GBT performance requirements at these frequencies are summarized in Table 1. Table 2 lists the sensitivity of pointing to errors in individual GBT components (Norrod & Srikanth 1996) to indicate the dimensional accuracies required for good performance at short wavelengths. The coordinates (X, Y, Z) in Table 2 originate at the vertex of the parent paraboloid, Z is the symmetry axis of that paraboloid, the X axis is horizontal, and the vertical (Y, Z) plane bisects the GBT primary. The tolerance ϵ in Table 1 would be the rss of errors in the primary and secondary surfaces if the telescope were perfectly collimated. Decollimation also contributes to ϵ, but the focal ellipsoid is large enough that ϵ is relatively insensitive to small collimation errors. Moving the secondary reflector in the Y_s causes axial defocusing, but the range between half-power (-3 db) points in telescope gain is fairly large, about 3.9λ (Srikanth 1990b). Transverse motion of the secondary in the elevation plane (caused by gravitational bending of the feed arm, for example) over a 3.4λ range only lowers the gain by 20% (-1 db) (Srikanth 1990a). The contribution of small feed motions to ϵ is negligible at the large $f/d = 1.9$ field-of-view at the secondary focus.

Note that the scientific performance requirements actually include *all* sources of error affecting an astronomical observation, not just those attributable to the telescope alone. For example, the rms (root mean square) tracking error σ_2 is really the rss (root sum square) of tracking errors caused by the GBT itself, uncertainties in the positions of pointing calibrators used for offset pointing, and errors in corrections for atmospheric refraction. Uncertainties in flux-density scales and atmospheric extinction will contribute to the rss flux errors. To ensure that the GBT is scientifically useful at high frequencies and to specify technical requirements for the GBT PTCS, we must at least understand the "non-PTCS" error components quantitatively. Even better, we should try to minimize them.

Table 1. GBT Scientific Requirements

ν (MHz)	tracking σ_2 ($f < 0.2$) (arcsec)	blind σ_2 ($f < 0.43$) (arcsec)	ϵ (mm)
52	2.8	6.1	0.36 ($\lambda/16$)
92	1.6	3.5	0.21 ($\lambda/16$)
115	1.3	2.8	0.21 ($\lambda/(4\pi)$)

Table 2. GBT Pointing Coefficients

Component Motion	Effect on Pointing
Primary focal length increase	-1.9 arcsec mm^{-1}
Primary Y rotation	$+1.77$ arcsec arcsec^{-1}
Primary X translation	$+2.7$ arcsec mm^{-1}
Primary Y translation	-1.9 arcsec mm^{-1}
Primary Z translation	-1.9 arcsec mm^{-1}
Subreflector X translation	-3.8 arcsec mm^{-1}
Subreflector Y translation	$+2.9$ arcsec mm^{-1}
Subreflector Z translation	$+2.1$ arcsec mm^{-1}
Subreflector X rotation	$+0.15$ arcsec arcsec^{-1}
Subreflector Y rotation	$+0.13$ arcsec arcsec^{-1}
Feed X translation	$+1.05$ arcsec mm^{-1}
Feed Y translation	-1.05 arcsec mm^{-1}
Feed Z translation	-0.25 arcsec mm^{-1}

REFERENCES

Balser, D. S., Maddalena, R. J., Ghigo, F., & Langston, G. I. 2002a, GBT Com Memo 17

Balser, D. S., Maddalena, R. J., Ghigo, F., & Langston, G. I. 2002b, GBT Com Memo 20

Condon, J. J. 1997, PASP, 109, 166

Condon, J. J., Cotton, W. D., Greisen, E. W., Yin, Q. F., Perley, R. A., Taylor, G. B., & Broderick, J. J. 1998, AJ, 115, 1693 (NVSS)

Condon, J. J., & Yin, Q. F. 2001, PASP, 113, 362

Hall, R., Goldman, M. A., Parker, D. H., & Payne, J. E. 1998, GBT Memo 191

Lockman, F. J. 1998, GBT Memo 192

Norrod, R., & Srikanth, S. 1996, GBT Memo 155

NRAO Newsletter 2000, 83, 5

Ruze, J. 1996, Proc. IEEE, 54, 633

Srikanth, S. 1990a, GBT Memo 48

Srikanth, S. 1990b, GBT Memo 49

This preprint was prepared with the AAS LaTeX macros v5.0

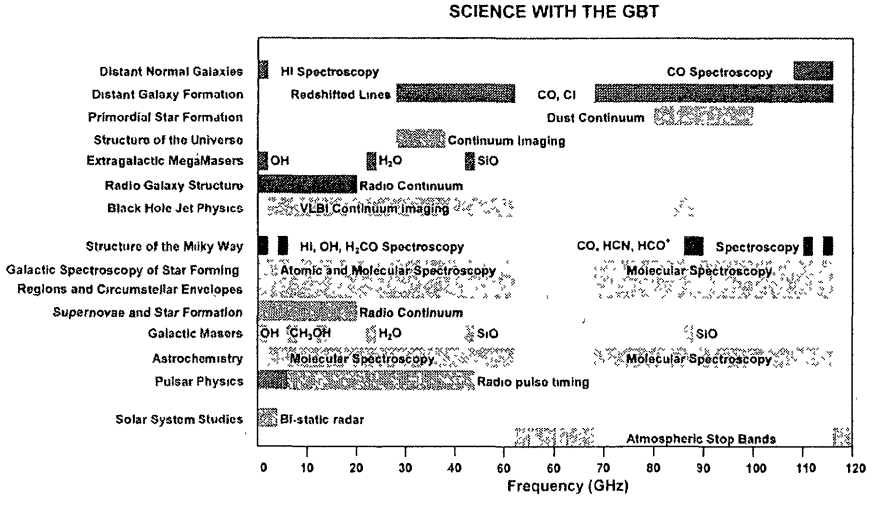

Fig. 1.— Frequency coverage of GBT science (NRAO 2000). Abscissa: Frequency (GHz).

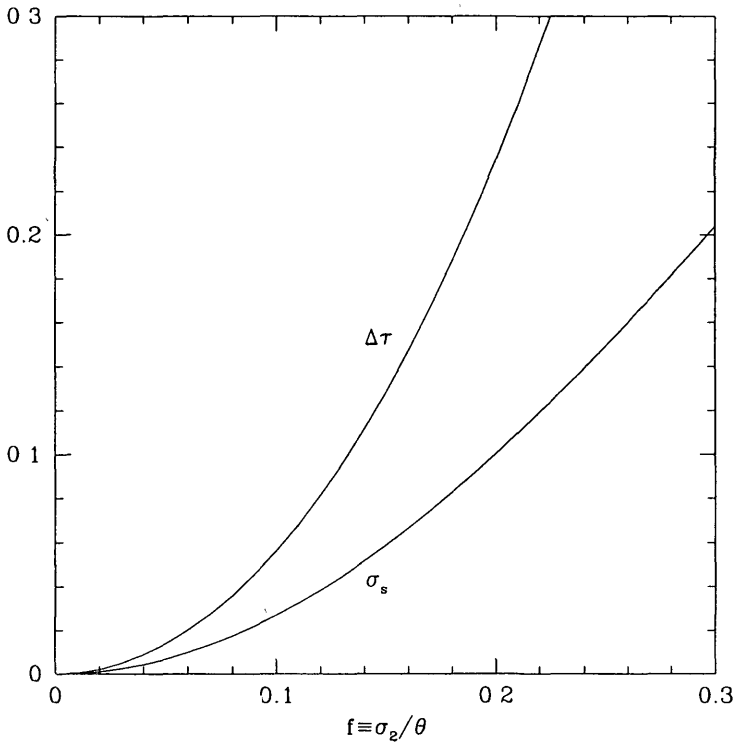

Fig. 2.— Tracking errors cause a sensitivity loss that may be compensated for by increased integration, and they cause flux-density calibration uncertainties. Abscissa: RMS tracking error in beamwidths $f = \sigma_2/\theta$ (dimensionless). Ordinates: Fractional flux error σ_s and fractional increase in integration time $\Delta\tau$ needed to compensate for sensitivity loss (dimensionless).

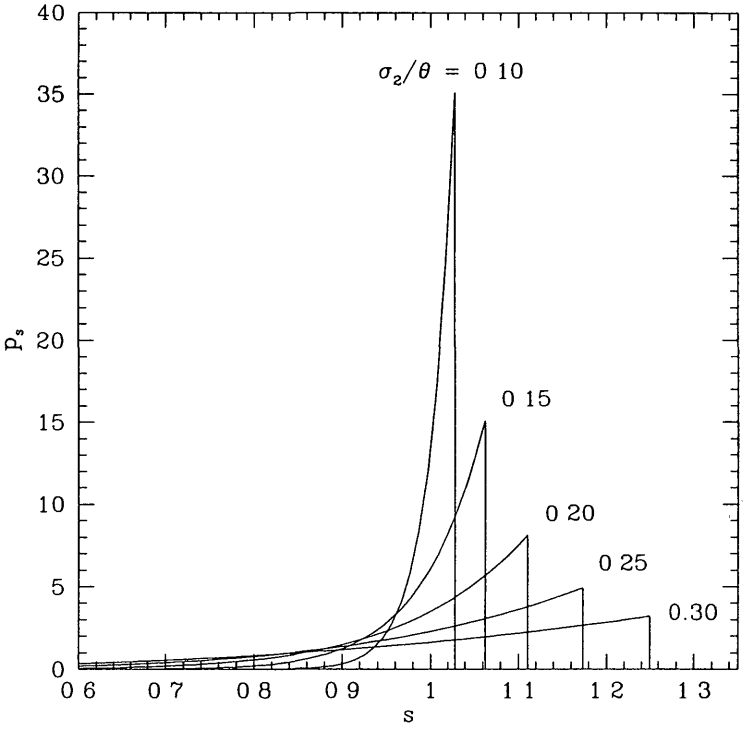

Fig. 3.— Distributions of the intensity-proportional flux error caused by pointing errors. Abscissa: Ratio s of observed to true flux density (dimensionless). Ordinate: Probability p_s (dimensionless). Parameter: RMS tracking error in beamwidths $f = \sigma_2/\theta$ (dimensionless).

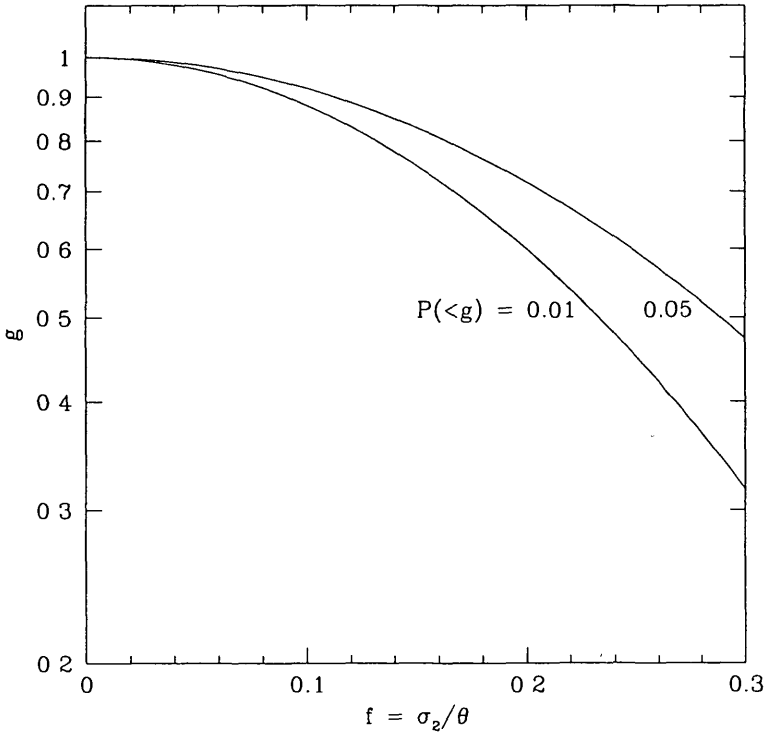

Fig. 4.— The sensitivity of detection experiments can be greatly reduced by large pointing errors. Abscissa: RMS tracking error in beamwidths $f = \sigma_2/\theta$ (dimensionless). Ordinate: Relative gain (dimensionless). Parameter: Probability $P(< g)$ of encountering a lower relative gain.

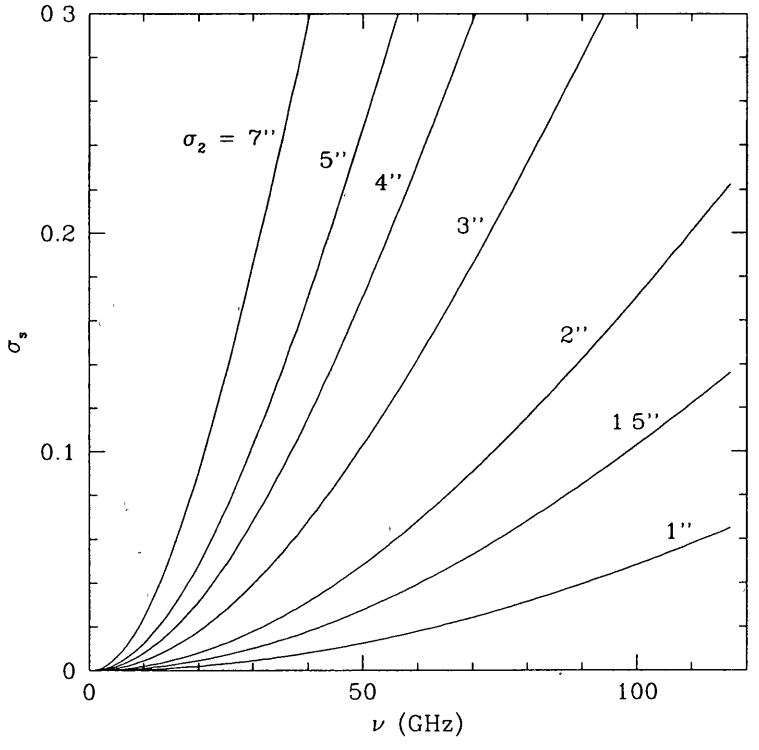

Fig. 5.— The most important effect of tracking errors is an intensity-proportional flux uncertainty. The rms fractional uncertainty σ_s for the GBT is shown as a function of frequency for several values of the rms tracking error σ_2. Abscissa: Frequency (GHz) Ordinates: RMS fractional flux uncertainty σ_s (dimensionless). Parameter: RMS tracking error σ_2 (arcsec).

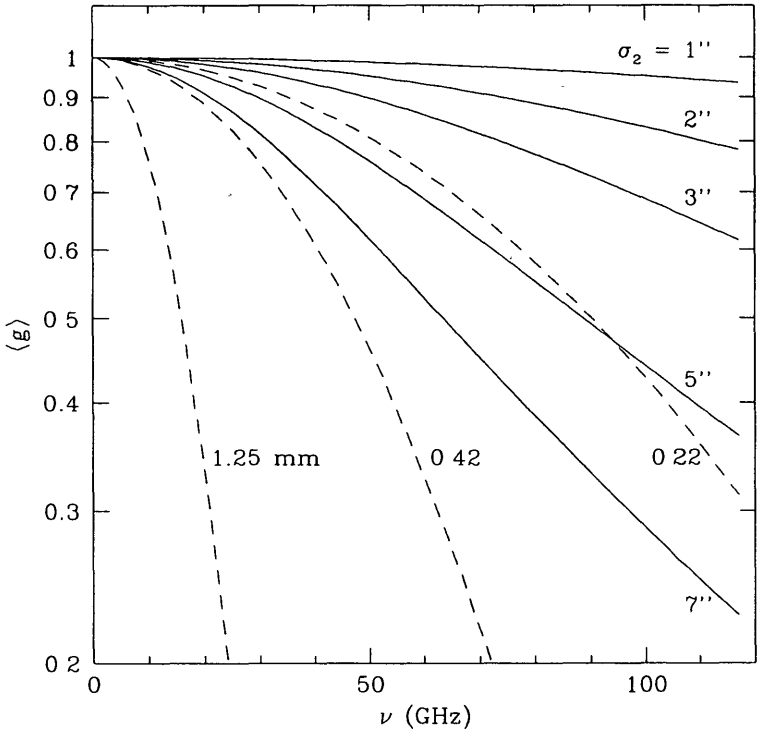

Fig. 6.— Tracking errors reduce the average on-source gain $\langle g \rangle$ of the GBT. The solid curves show $\langle g \rangle$ as a function of frequency for several values of the rms tracking error σ_2. For comparison, the dashed curves show the surface efficiency η as a function of frequency for several values of the rms surface error—1.25 mm, 0.42 mm and 0.22 mm correspond to the Phase I, II, and III expected errors (Hall et al. 1993). It appears that surface errors will have a much larger effect than pointing errors on the average on-source gain of the GBT. Abscissa: Frequency (GHz) Ordinates: Relative gain (dimensionless)

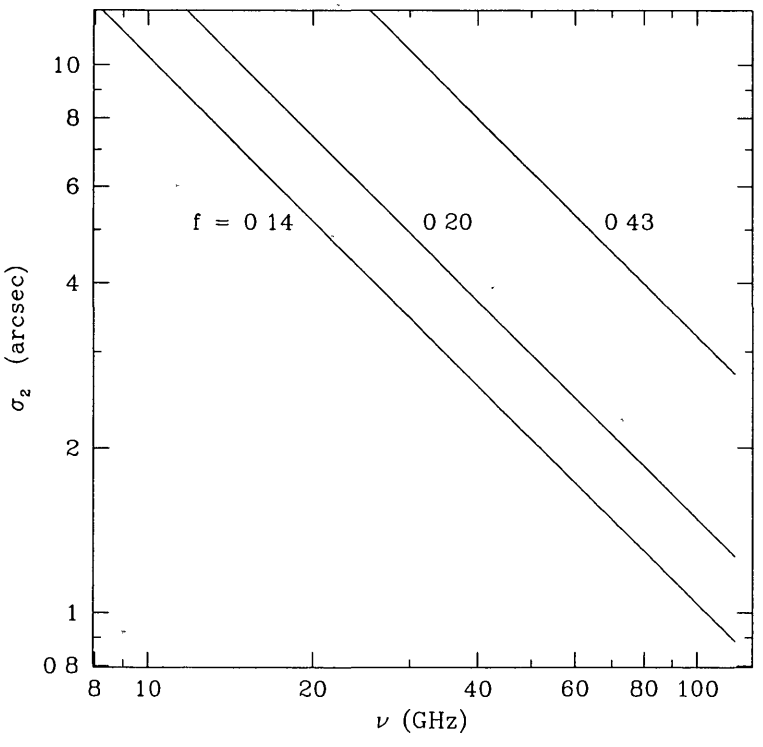

Fig. 7.— The rms pointing errors σ_2 needed for accurate tracking ($f = 0.14$), adequate tracking ($f = 0.20$), and blind pointing ($f = 0.43$) with the GBT are shown as functions of frequency. Abscissa: Frequency (GHz) Ordinate: RMS pointing error σ_2 (arcsec)